Optimal Measurement of Surface Shortwave Irradiance Using Current Instrumentation

J. MICHALSKY,* E. DUTTON,+ M. RUBES,# D. NELSON,+ T. STOFFEL,@ M. WESLEY,&
M. SPLITT,** AND J. DELUISI++

* *Atmospheric Sciences Research Center, The University of Albany, State University of New York, Albany, New York*
+ *Climate Monitoring and Diagnostics Laboratory, National Oceanic and Atmospheric Administration, Boulder, Colorado*
# *Cooperative Institute for Research in Environmental Studies, Boulder, Colorado*
@ *National Renewable Energy Laboratory, Golden, Colorado*
& *Environmental Research Division, Argonne National Laboratory, Argonne, Illinois*
** *Cooperative Institute for Mesoscale Meteorological Studies, University of Oklahoma, Norman, Oklahoma*
++ *Surface Radiation Research Branch, National Oceanic and Atmospheric Administration, Boulder, Colorado*

(Manuscript received 7 July 1997, in final form 16 February 1998)

ABSTRACT

Although most measurements of total downwelling shortwave irradiance are made with pyranometers, the World Climate Research Program's Baseline Surface Radiation Network has recommended the use of the summation of shortwave components in which the direct normal irradiance is measured and multiplied by the cosine of the solar zenith angle and then added to the diffuse horizontal irradiance measured by a pyranometer that is shaded from direct solar radiation by a disk. The nonideal angular response of most pyranometers limits their accuracy to about 3%, or 20–30 W m^{-2}, for instantaneous clear-sky measurements. An intensive study of 21 separate measurements of total horizontal irradiance was conducted during extreme winter conditions of low sun and cold temperatures over 12 days at the National Oceanic and Atmospheric Administration's Climate Monitoring and Diagnostics Laboratory. The experiment showed that the component sum methodology could lower the uncertainty by a factor of 2 or 3. A clear demonstration of this improvement was realized in a separate experiment conducted at the Atmospheric Radiation Measurement Southern Great Plains Cloud and Radiation Testbed site during April 1996. Four independent measurements of downwelling shortwave irradiance using the component sum technique showed typical differences at solar noon of about 10 W m^{-2}. The mean of these summed measurements at solar noon was lower than the mean of the most-well-calibrated pyranometer measurements, acquired simultaneously, by about 30 W m^{-2}, which is consistent with the typical angular response of many pyranometers.

1. Introduction

Several studies show that clear-sky, shortwave (solar) models of surface irradiance overestimate measurements. Betts et al. (1993) used the European Centre for Medium-Range Weather Forecasts (ECMWF) shortwave model to calculate surface irradiances that were 5%–10% higher than measurements for clear skies during the First ISLSCP (International Satellite Land Surface Climatology Project) Field Experiment (FIFE) in Kansas. Wild et al. (1995) used a different formulation of the ECMWF shortwave model but found that the model overpredicted clear-sky, shortwave Global Energy Balance Archive (GEBA) measurements by an average of 3%. Charlock and Alberta (1996) used meteorological data from the Atmospheric Radiation Measurement (ARM) program as input to the Fu and Liou (1993) radiation code and then compared to ARM surface radiation measurements. The Fu–Liou code overestimated midday, clear-sky, shortwave irradiance by between 3% and 4%. Ding and Wang (1996) also used data from the ARM program and found that the GENESIS shortwave general circulation model, likewise, overpredicted clear-sky irradiance by about 4%.

Recently, others have suggested that there is no clear evidence that shortwave irradiance is overpredicted by models. Cess et al. (1996) compared the National Center for Atmospheric Research's Community Climate Model (CCM2) with measurements made at the surface and at the top of the atmosphere near the Boulder Atmospheric Observatory. Cess et al. (1996) found that the clear-sky absorption indicated by differencing satellite and ground-based net flux measurements agreed with the prediction of the CCM2 model. Zender et al. (1997) used a new shortwave code to calculate total horizontal irradiance for clear skies during the ARM Enhanced Shortwave Experiment in October 1995 in Oklahoma. Their model results were slightly higher than noontime irradiance measurements but were clearly within the un-

Corresponding author address: Joseph Michalsky, Atmospheric Sciences Research Center, The University of Albany, State University of New York, 251 Fuller Road, Albany, NY 12203.
E-mail: joe@asrc.cestm.albany.edu

certainty set by those measurements and the inputs needed for the model.

These analyses indicate an inconsistent picture of surface shortwave irradiance measurements and models that may be related to the irradiance measurements, to the measurement of the model inputs, or to the models themselves. Kato et al. (1996) compared three observations of total horizontal irradiance made at the Southern Great Plains (SGP) ARM site near Lamont, Oklahoma, with model calculations using the delta two-stream model of Toon et al. (1989). The most realistic (mineral dust) aerosol model overpredicted surface shortwave irradiance for clear skies. However, the measurements disagreed among themselves by as much as the nearest measurement to this model result disagreed with this model.

Two independent, but related, intensive measurement programs were conducted that help resolve this measurement disparity. 1) An experiment was conducted at the National Oceanic and Atmospheric Administration (NOAA) Climate Monitoring and Diagnostics Laboratory (CMDL) to assess the accuracy and precision of current off-the-shelf shortwave instrumentation in the extremely difficult situation of low-sun early-winter conditions, with careful attention to maintenance during the test. 2) Reference instruments were deployed in April 1996 at the SGP ARM site central facility near the two standard shortwave measurements stations that operate there continuously. We begin with an extended discussion of the CMDL experiment. Next, the specifics of the experiment at the ARM SGP site are described, including a description of instrumentation and a description of specific measurements made. The results are summarized and discussed in the final section.

2. CMDL test of commercial instrumentation

Flowers and Maxwell (1986) (and E. C. Flowers (1997, personal communication) describe the component summation method as the preferred measurement of total (global) horizontal irradiance. Formally, the World Climate Research Program's Baseline Surface Radiation Network (BSRN) specifies that total horizontal irradiance will be measured as the sum of its components—that is, the vertical component of the direct normal irradiance (hereafter, the direct horizontal irradiance) measured by a tracking pyrheliometer (preferably, an absolute cavity radiometer) and the diffuse horizontal irradiance measured by a pyranometer whose dome and receiver are shaded by a tracking disk (Ohmura et al. 1998).

To evaluate this procedure's accuracy for standard off-the-shelf instrumentation, in the most challenging portion of the annual cycle, winter's low sun angles, an experiment was conducted at CMDL in December 1996 and January 1997.

a. Background

Thorough characterizations of the pyranometers widely used for observations of total solar irradiance often reveal a varying sensitivity to irradiance as a function of incident angle, commonly called the ''cosine response error.'' The fact that this variation can be detrimentally large and often not accurately determined can lead to large uncertainties and disappointing discrepancies among observations. The problem of cosine errors in pyranometers has led some insightful investigators to use the sum of separately measured direct and diffuse irradiance as an alternative method that is mostly free of the cosine error limitation (Flowers and Maxwell 1986; Ohmura et al. 1998). To evaluate the performance of this component sum technique for obtaining total solar irradiance observations, a comparison between the alternative techniques using a diverse group of radiometers was performed. Several models of pyranometers and pyrheliometers from five different manufacturers and multiple absolute cavity radiometers traceable to the World Radiometric Reference (WRR) (Fröhlich 1978) were used. The comparison period was 12 days near the winter solstice in Boulder, Colorado (40.0°N), when observing conditions are most adverse for the year because of low sun angles, temperature extremes, and potential icing on the optical surfaces, all of which tend to amplify observational errors. Using these observations, various methods of obtaining total solar irradiance were compared to a specific reference observation. The primary emphasis of this comparison was to evaluate different representative instruments and techniques relative to this reference observation. To answer the question of the absolute accuracy of the different instruments and techniques, it is imperative to know the reference accuracy. For this reason, the comparison reference was designed to be as accurate as possible.

b. Instruments

This observational comparison consisted of solar irradiance observations with nine pyrheliometers of three different designs from two manufacturers, nine shaded pyranometers of six different designs from four manufacturers, 14 total pyranometers of nine designs from five manufacturers, and five ambient temperature electrical-substitution cavity radiometers (ESCRs) of three designs from two manufacturers. The instrument manufacturers and models used for this test are listed in Table 1. All instruments incorporated thermopile or precision resistance thermometer (PRT) heat sensor technology for the detection of solar radiation. In an effort to include a broadly representative group of instruments in this comparison, there was no preselection of instruments as might typically occur before any of these instruments would be deployed for routine field service. By not selecting instruments, the group represents instruments that might have been in the field for an ex-

TABLE 1. Instruments used in CMDL test.

Total pyranometers	Diffuse pyranometers	Direct pyrheliometers	Cavity radiometers
Eppley Models			
PSP	PSP	NIP/5.7	AHF
Type D TP	Model 2	NIP/5.0	Eppley–Kendall
Model 2			
FPP			
Kipp and Zonen Models			
CM-10	CM-11	CH-1	
CM-21	CM-21		
EKO Model			
801	801		
Yankee Environmental Systems, Inc. Model			
TSP-700			
Spectrolab (no serial number)	Spectrolab (no serial number)		Technical Measurements, Inc. (no serial number)

tended period of time as well as more recently calibrated instruments. Therefore, the results of the comparison of all included instruments cannot be considered indicative of the true capabilities of the technology. This is better demonstrated in the following comparison analysis when a subgroup of selected instruments is used. The purpose of the comparison was to compare observational techniques and representative instruments; therefore, individual instrument makes and models are not identified in the results given in the rest of this section.

Instrument detector viewing geometry is particularly important in defining both the direct beam and diffuse measurement. The field of view of the direct beam instruments is defined by an aperture at the end of a tube forward of the detector. This field of view is larger than the apparent diameter of the sun to allow for historic variations in tracking capabilities. Important geometrical considerations in determining total solar irradiance from the sum of diffuse and direct are the equality of angles subtended by the aperture of the direct and the tracking disk for the diffuse, and the proper alignment of both. With the typical subtended angle for both being about 5°, any excess energy captured by the direct measurement due to forward scattered radiation around the solar disk is compensatingly blocked from the diffuse measurement. The function of the solar tracking mechanisms are to keep both devices tracking such that the sun is centered to within 0.1° of the true center of the field of view. Some of the direct beam and diffuse instruments used here had slightly varied geometries for the purpose of detecting any related effect: none was found, primarily because the variations were small, amounting to about 0.7° in the subtended angle.

c. Measurements

The observations were carried out using the facilities and resources of the CMDL's Solar Radiation Facility. Measurements were made nearly simultaneously on all instruments every 10 s for 12 days in December 1996 and January 1997. The radiometers were located on the roof of an eight-story building in central Boulder and had a largely unobstructed view of the sky, with the exception of mountains to the west subtending an elevation angle of generally less than 5° and minor towers and structures projecting a few degrees above the horizon. The only obstructions affecting the direct beam were the mountains, where this time of year the sun set behind the highest peak, reaching 8.5° above the horizon. All instruments were located in close proximity, within a 6-m radius, so that all obstructions had nearly equal impact on all instruments and did not affect the comparison. The six solar trackers used to aim direct beam instruments at the sun and continually align shade disks for diffuse pyranometers have demonstrated tracking accuracy of 0.1°, which is sufficient to minimize any tracking-related errors in instrument-to-instrument comparisons. The instruments and trackers received close attention during the comparison period to verify proper continuous operation. Each ESCR was internally and automatically calibrated every 30 min on a staggered schedule, so that only one instrument at a time would be in the ESCR's calibration mode, which extends for approximately 3 min. Continuous operation of the ESCRs required extra attention because the ESCRs lack all-weather operation capability. During precipitation, the ESCRs, whose internal cavity is pointed directly at the sun, need to be covered, and the signal for the reference observation is lost, which is generally of little consequence, since there is little or no direct beam during precipitative conditions. A total of 11 clocks used to time the ESCRs, trackers, and dataloggers were synchronized to within 1 s each morning during the comparison, and they varied by fewer than 2 s during the rest of each day.

d. Reference measurement

The reference irradiance observation to which all others are compared is intended to be as near truth as pos-

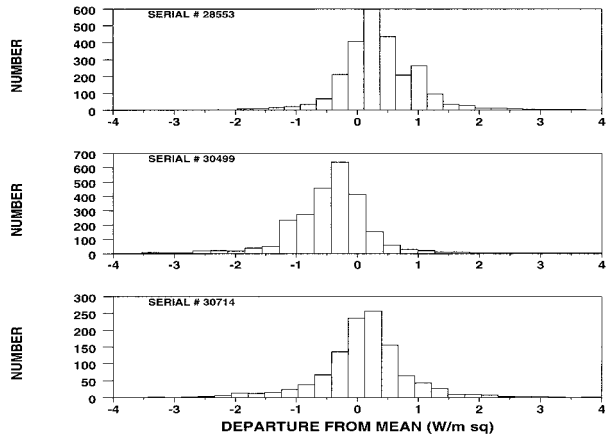

FIG. 1. Histogram of differences in watts per square meter between 10-s readings for each cavity and the mean of three cavities. The mean difference between cavities is 0.3 W m^{-2} with 99% of all readings within 1.5 W m^{-2}.

sible. For this comparison, a reference observation was chosen to be the average of two or three ESCRs, depending on their calibration cycles, with each corrected to the WRR (Fröhlich 1978) scale plus the average of nine diffuse radiometers. The ESCRs used for daily observations were automatic Hickey–Frieden absolute cavity radiometers, serial numbers 28553, 30499, and 30714. Each of these units has an associated WRR correction factor that was applied to normalize each instrument's output to WRR scale values. These factors were 0.99756, 0.99915, and 0.99732. Figure 1 shows a comparison of each of the three cavities to the mean of the group for one day of the comparison. The mean difference is less than 0.3 W m^{-2} with a full range (99%) of less than ± 1.5 W m^{-2} among the group of cavities. Two other cavities help establish the reference measurement by serving as long-term ''shelf'' standards to which the other three are periodically compared.

The error in the reference total irradiance is a combination of the error in the direct beam and that in the measured diffuse. There is no widely recognized calibration reference standard for diffuse irradiance. Typically, the WRR calibration scale is transferred to a diffuse pyranometer when the direct beam incident angle on a pyranometer is near 45°. Although not exact, this angle is considered to be the mean incident angle of diffuse irradiance. Errors in the diffuse may result, from anisotropic diffuse fields to the extent that the sensor has a cosine response error, instrument nonlinearity since intensity levels vary by as much as an order of magnitude from the calibration levels, errors in the 45° normalization/calibration procedure, and the inherent limitations of thermal-based irradiance sensors. To the extent that there are random or offsetting components in and between some of these errors, an improved instantaneous diffuse is obtained by averaging multiple independent observations—in this case from the nine shaded pyranometers. Errors in the diffuse measurements have a diminished impact on the clear-sky determination of total irradiance because frequently less than 15% of the total irradiance is due to the diffuse component. The reference observation resulting from the sum of the average of the cavities and the average of the shaded pyranometers is taken as the most accurate possible representation of actual total irradiance. An analysis of the possible sources of absolute error in this reference suggests that the total error is about 4 W m^{-2}. A diffuse larger than 15% would, of course, increase this error proportionately.

e. Observational results

A wide variety of sky conditions existed during the 12 days of the comparison. A summary of all 12 days irradiance values is given in Fig. 2, in which samples of direct, diffuse, and total irradiance values are plotted for the 12 days. Approximately one-third of the data shown can be classified as either clear, partly cloudy, or overcast.

Figure 3 uses data for the cloud-free day denoted DOY4 in Fig. 2. This figure shows the maximum differences for the diffuse horizontal, the direct horizontal, the total horizontal based on a single pyranometer measurement, and the total horizontal based on the component sum. These curves depicting ranges were smoothed from the original 10-s data using a 45-min running average. The lines in Fig. 3 represent the spread of results that are obtained for this particular group of unselected instruments. The solid line is the range in the total horizontal irradiance based on unshaded pyranometer measurements. This should be compared with the dot–dash line where the total is based on summing direct and diffuse components. This dramatically demonstrates the cosine response differences among the unshaded pyranometers. The dotted line is the range of the diffuse measurements made with shaded pyranometers, and the dashed line is the range in the direct component that is measured with the pyrheliometers and multiplied by the cosine of the solar zenith angle.

The observational data were merged from five dataloggers and edited to remove any data adversely affected by obstructions, tracker adjustments, instrument cleaning, or inadvertent shadowing. The most recently available linear calibration constant was applied to the voltages of all pyranometers and pyrheliometers to derive irradiance in watts per square meter. Solar zenith angles were computed for every 10 s to allow the direct horizontal irradiance to be calculated. Each of the nine diffuse readings was added to each of the nine pyrheliometer's direct horizontal irradiances for nine independent determinations of total irradiance. In all, 21 independent simultaneous observations of total irradiance were determined from the test instrument group every 10 s for the entire 12 days. With the 1/*e*-folding time of the instruments on the order of 1–2 s, the 10-s interval between readings produced truly independent

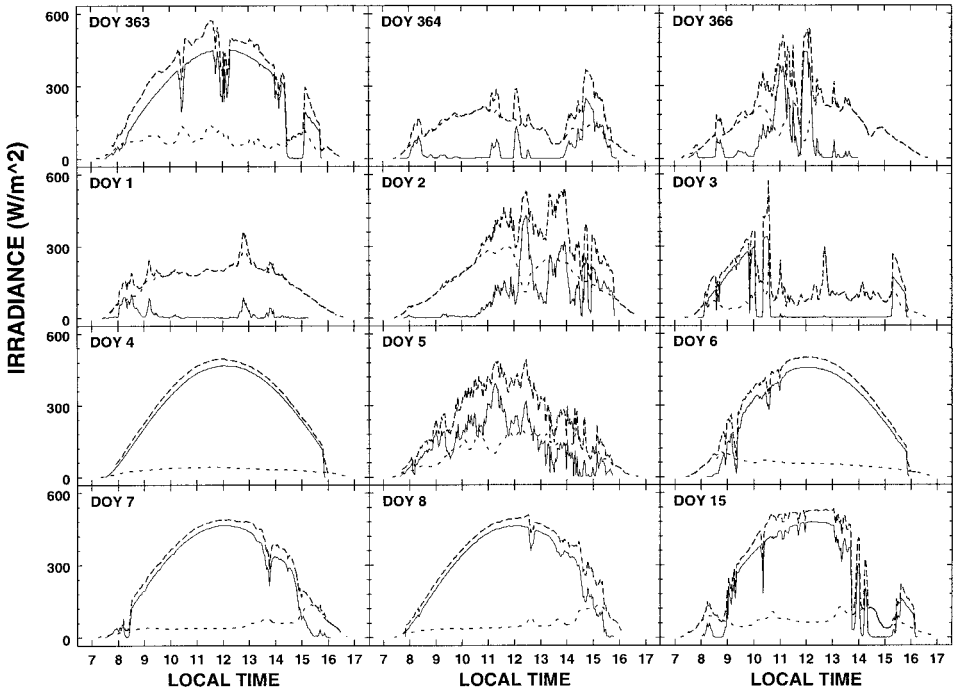

FIG. 2. Direct horizontal (solid), diffuse horizontal (light dash), and total horizontal (heavy dash) solar irradiance for 12 days of test. DOY is the day of year in late 1996 or early 1997.

readings, although, a 1-Hz sampling rate is recommended for radiation monitoring to ensure accurate energy integral estimates as required for BSRN measurements (Ohmura et al. 1998). Even though all instruments were sampled within ± 1.5 s of each other, the rapidly varying irradiance field during broken cloud conditions and the response time of the instruments will result in different readings that typically cancel with sufficient averaging but will show up in a comparison of the instantaneous values.

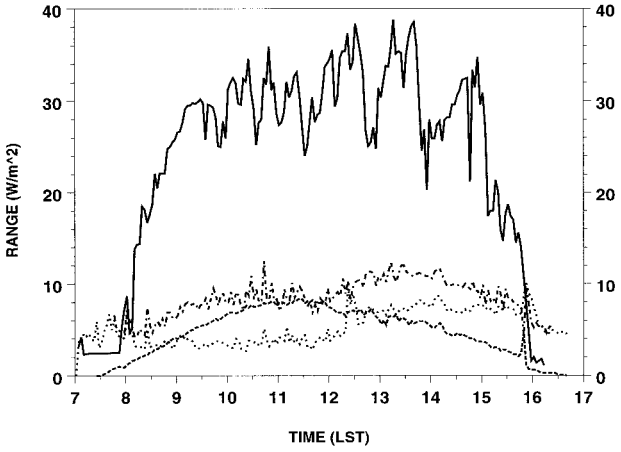

FIG. 3. The range of different measures of irradiance on a clear day (1 April 1997): Solid—pyranometer total; dash–dot—total using sum; dotted—diffuse; dashed—direct horizontal. Range curves smoothed with 45-min running average.

f. Comparison results

The basic comparison procedure was to take the difference between each of the 21 independently determined 10-s total solar irradiances and the reference value. These differences can then be examined in a histogram representation for each instrument or instrument combination and the relative performance of each compared. Figure 4 shows the ''error'' histograms of the 12 unshaded pyranometers, and Fig. 5 shows the same for the nine component sums, where each histogram is an accumulation of the 12 days where the errors were grouped in 0.1 W m^{-2} bins. Note that there is quite a range of results for the individual pyranometers—from a relatively narrow clustering about the zero value to wide excursions and bimodal characteristics. The component sum differences in Fig. 5 display a far more consistent behavior (note change is abscissa scale) having a single mode with means within 5 W m^{-2} of zero. Although it is apparent that the mean for the component sums should lie closer to the zero value since the average of their diffuse component makes up a portion of the reference value, the difference in the shape and spread of the errors in Fig. 5 relative to Fig. 4 reveals the improved capability of the component sum approach. For this analysis, a third type of total irradiance determination was also formulated, as recommended by the BSRN, by adding each of the diffuse irradiances to one of the ESCRs to simulate the most accurate instrument pair measurement that might be deployed for routine field use. The use of an ESCR for measuring the direct

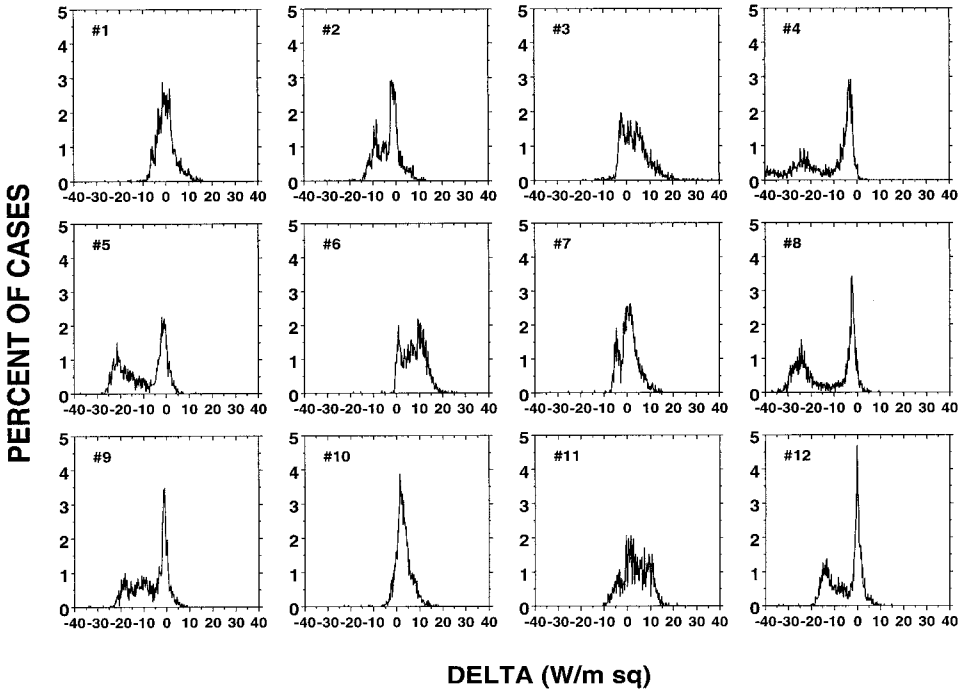

FIG. 4. Histograms (0.1 W m^{-2}) of differences between each of the total pyranometers and the reference measurement. Twelve days of data (10-s intervals). Note obvious bimodal behavior of numbers 4, 5, 8, 9, and 12.

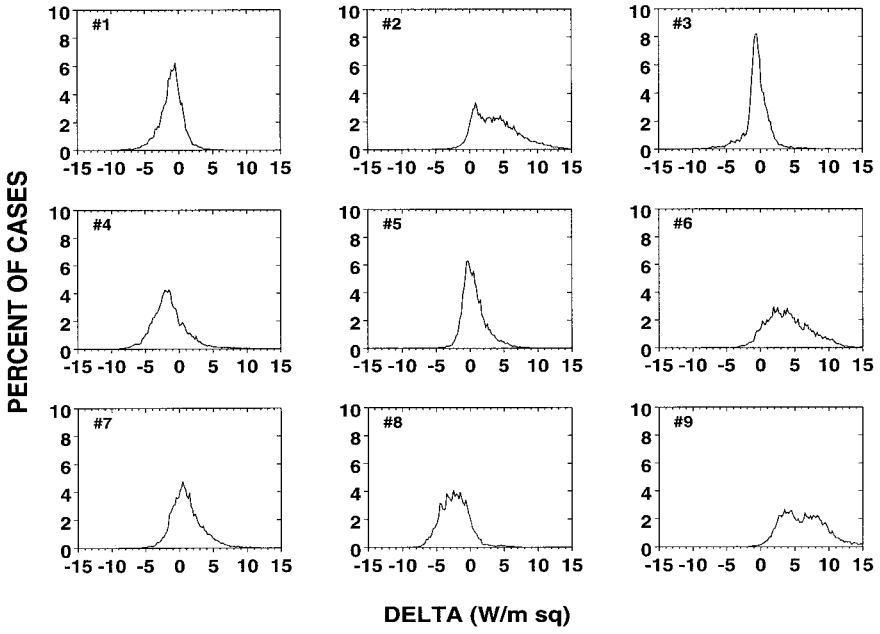

FIG. 5. Histograms (0.1 W m^{-2}) of differences between each of the total measurements based on sums and the reference measurement. Twelve days of data (10-s intervals). Note more symmetrical distributions compared to Fig. 4.

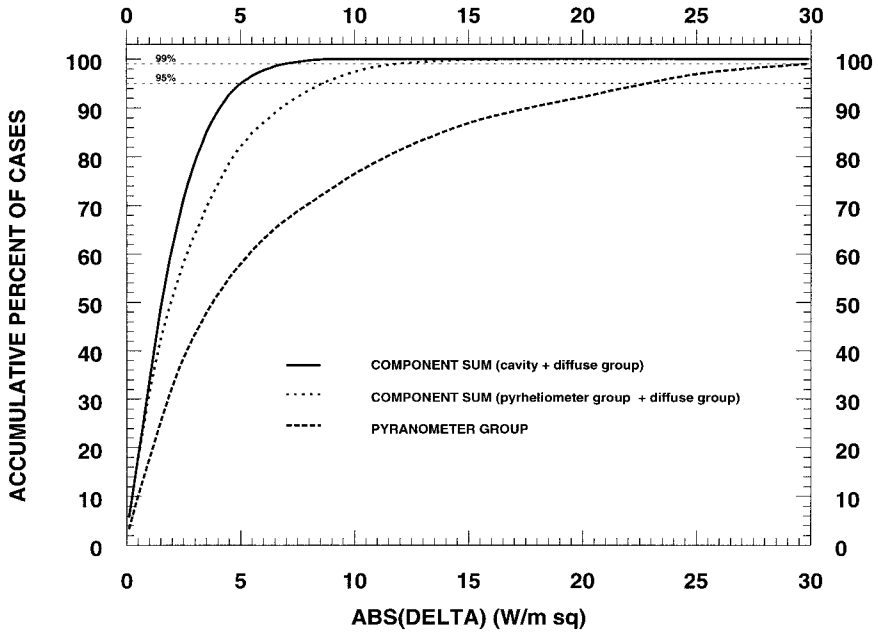

FIG. 6. Cumulative distributions for three different measures of total horizontal irradiance differenced with a reference measurement based on 10-s samples over 12 days. Note improvement of sums over single instrument.

beam component of the component sum improves the result by not introducing the errors that propagate from first calibrating the windowed pyrheliometer relative to the ESCR.

To readily determine and display the total percentage of measurements for each different instrument or instrument combination that falls within a certain error range, cumulative probability distributions were computed. This approach was used instead of simply computing standard deviations because of the nonnormal distribution demonstrated by a number of error distributions (see Figs. 4 and 5). The three cumulative absolute error probability distributions are seen in Fig. 6 for all edited 10-s samples, for all instruments, and for all sky conditions. These distributions are obtained by determining the relative frequency of occurrence of errors smaller than an ever-increasing value for a specific set of observations. The 95% and 99% lines are included for reference. A notable improvement in performance is indicated when moving from the pyranometer group to the pyrheliometer component sum group to the single cavity component sum group. This improvement is due, in large degree, to the significant reduction in the cosine error that occurs under clear skies in the pyranometers and to the elimination of the additional errors that occur in a group of pyrheliometers relative to those of a cavity. This second point would be better illustrated if an equal number of cavities had been used, but Fig. 1 is indicative of the mean difference and spread between cavities for instantaneous measurements, such that a comparison with nine cavities would yield similar results to the current one.

Identifying the cosine response as the major cause of error is further substantiated when examining the cumulative error distributions in which the analysis distinguishes between clear, overcast, and partly cloudy skies, as in Fig. 7. The instruments included in the analysis in Fig. 7 were selected to eliminate a few instruments in each group that demonstrated anomalous characteristics in the sense that they may not have been chosen for field deployment by a discerning analyst. However, that selection does not affect the following analysis relative to clouds.

In Fig. 7 note that in the extended absence of the direct beam, that is, overcast conditions, the pyranometer group agrees with the component sum group at about the same error level as the component sum demonstrates under clear skies. This suggests that even though the component sum was somewhat biased to better agreement with the reference, the unshaded pyranometers do agree with the mean of the shaded ones to within about 7 W m^{-2} when the irradiance is entirely diffuse. This tends to confirm that the major cause of the relative poor performance of the unshaded pyranometers as a group is due to the error introduced by the direct solar beam, especially at these larger zenith angles experienced during winter. It should be noted that different instruments have different cosine responses. In addition, if it can be shown that a given pyranometer has very small to negligible cosine error, the pyranometer can produce results nearly as accurate as the component sum. In Fig. 7 the clear-sky case for the pyranometer group is the worst case and that the broken-cloud case is intermediate.

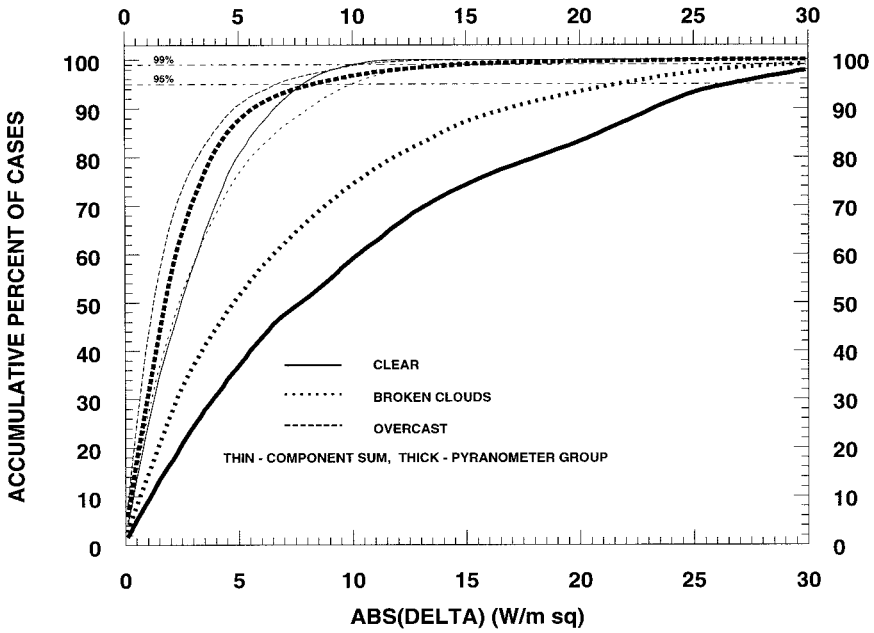

FIG. 7. Cumulative distributions of differences of total from single instrument and total based on sum from the reference total for clear, broken cloud, and overcast conditions. Note single instrument improvement for overcast.

An estimate of the total absolute error for instantaneous observations in any of the methods described here is obtained for a given confidence level by adding the values read from the appropriate curve in Fig. 6 or Fig. 7 and by adding to that the uncertainty in the reference value, which is estimated to be about 4 W m^{-2}. The effects of averaging over time to reduce the difference errors was investigated by repeating some of the above analysis on 2-min averages of the 10-s data. This averaging generally had the effect of reducing the error and shifting the curves in Figs. 6 and 7 to the left by less than 1 W m^{-2}. Further averaging over time would further reduce the random errors and at certain times of the year would tend to reduce the cosine-response-related error since the instrument's linear calibration constant is normalized near the 45° incident angle. With this normalization angle, results from incident angles less than 45° compensate for incident angles greater than 45°, and daily and longer averages improve.

g. Conclusions

There is a notable improvement in the accuracy of instantaneous total solar irradiance when going from single pyranometers, typical of those widely used in the United States, to the component sum technique using otherwise similar radiometer technology. This improvement is nominally about 15 W m^{-2}, depending on the extent of the cosine error in the stand-alone pyranometer. Further improvements, 3–4 W m^{-2}, are realized when the pyrheliometer is replaced with an absolute cavity for the direct beam measurement. Going from instantaneous 10-s to 2-min averages of 10-s data resulted in less than 1 W m^{-2} improvement. This exercise demonstrates the limitations of typical ground-based thermal-sensing solar radiometry when it comes to efforts to measure the climatically important quantity of total solar irradiance. One of the most troublesome remaining limitations is that associated with the lack of a well-established calibration reference for diffuse sky irradiance. A relatively large uncertainty is therefore associated with the uncertainty assigned to the overall accuracy of the technique but it does not affect the conclusion as to the improvement achieved when using the component sum method. The component sum method does, unfortunately, complicate the routine measurement of total solar irradiance because of the need for a suitable tracking device, typically costing much more than the radiometric instrumentation and requiring line AC power. For critical research applications, particularly climate-related satellite and radiative transfer validation, the improved accuracy is critical and should be well worth the additional effort and expense.

3. ARM SGP April 1996 test

As explained in the introduction, these SGP measurements were initiated to resolve the disparities in total horizontal irradiance measurements made with single pyranometers. In fact, they served to demonstrate the performance of the component sum methodology in establishing a better, more consistent estimate of total horizontal irradiance, specifically at the SGP ARM site in northern Oklahoma in April 1996. In the previous

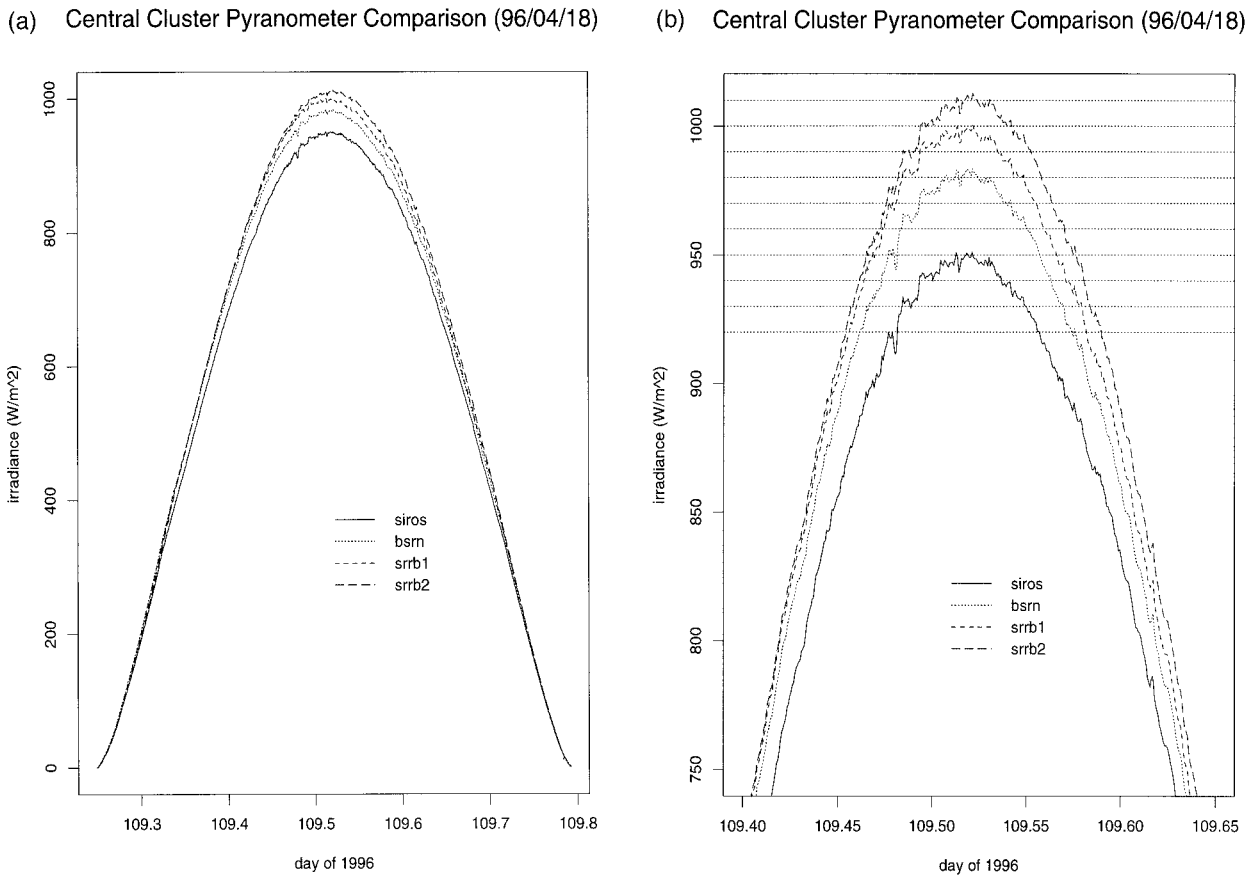

FIG. 8. (a) Total horizontal irradiance (four pyranometers). (b) Expanded scale of (a) near solar noon.

section, the measurements were carefully monitored with frequent checks throughout the day. In this experiment, two sets of measurements were made according to routine practice, and two sets of measurements were carefully monitored throughout the period with the constant oversight of an operator.

a. Instrumentation

Two sets of instruments are deployed continuously and side by side at the central facility near Lamont, Oklahoma. The standard set includes a pyranometer (The Eppley Laboratory, Inc., model Precision Spectral Pyranometer—hereafter Eppley PSP) measuring total horizontal irradiance, a pyranometer (Eppley PSP) under a tracking disk measuring diffuse horizontal irradiance, and a pyrheliometer (Eppley model Normal Incidence Pyrheliometer—hereafter, NIP) on the same tracker (Sci-Tec Model 2AP) measuring direct normal irradiance. There are two complete sets of these instruments within 5 m of each other. Total horizontal irradiance is measured directly with a pyranometer, and it is calculated by summing the diffuse horizontal irradiance and the direct horizontal irradiance.

To compare to the standard sets, two Eppley model AHF electrical-substitution cavity radiometers to measure direct normal irradiance were brought to the site from the Surface Radiation Research Branch (SRRB) of NOAA. SRRB also supplied selected Eppley PSP pyranometers for two total and two diffuse horizontal irradiance measurements. The trackers used for direct normal and diffuse horizontal irradiances were Sci-Tec Model 2AP trackers. The Atmospheric Sciences Research Center (ASRC) of the State University of New York supplied an Eppley NIP and an Eppley PSP that were calibrated the week before for direct normal and total horizontal irradiance measurements. The NIP was mounted on a LI-COR, Inc., model 2020 solar tracker.

Measurements were taken between 17 and 26 April 1996. Among the instrument mix, there were samples taken at 1-, 3-, 5-, and 20-s time steps. The comparisons that follow are based on 1-min averages of these samples. Mostly clear skies prevailed on 18, 19, and 23 April, and those data will be discussed here. The SRRB and ASRC equipment was deployed within 30 m of the two ARM standard shortwave sets.

b. Measurements

Total horizontal irradiance measurements from four pyranometers on 18 April appear in Fig. 8a. The irra-

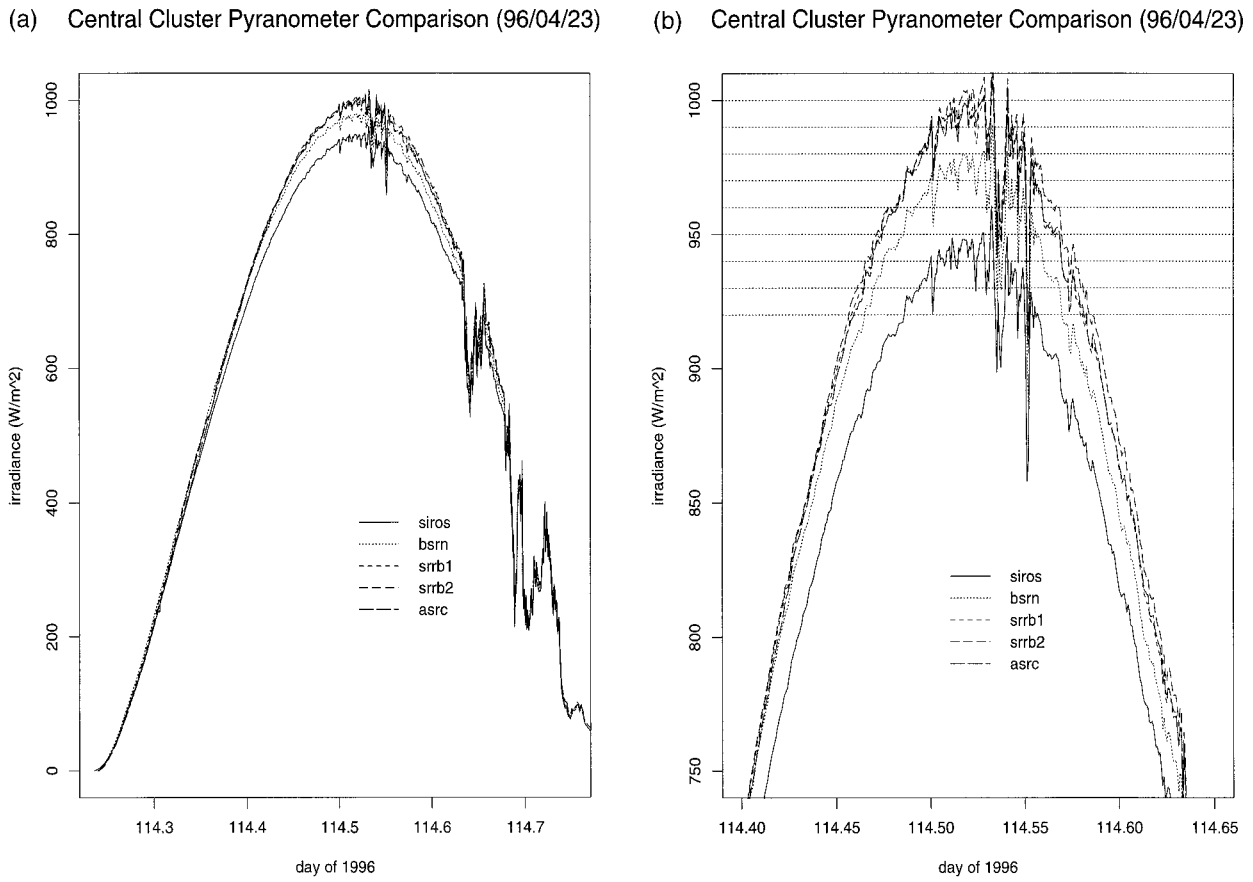

FIG. 9. (a) Total horizontal irradiance (five pyranometers). (b) Expanded scale for (a) near solar noon.

diance throughout the day is plotted versus local standard time. Since the SGP site is in the western part of the central time zone, solar noon occurs about one-half hour later than local noon. The day was cloud free, and the discrepancies in measurements are obvious, especially near solar noon. Figure 8b expands the scale of the solar noon portion of the plot in Fig. 8a and adds grid lines every 10 W m^{-2} to estimate the spread among instruments. The range in this set for this day near solar noon is 60 W m^{-2}. ''Siros'' refers to the Solar and Infrared Radiation Observing System, and ''bsrn'' refers to a duplicate set of measurements at the same location that were the first set deployed as part of the BSRN program. In fact, the data actually sent to the BSRN archive will likely contain data from either set of instruments. ''Srrb1'' and ''Srrb2'' refer to the two sets of SRRB instruments.

The srrb1 and srrb2 pyranometers were calibrated after they were brought back from Oklahoma in April 1996 at the National Renewable Energy Laboratory (NREL) using their BORCAL technique (Myers et al. 1989). The bsrn pyranometer used for total horizontal irradiance was calibrated 7 months before the measurements using the BORCAL method, and the remaining siros and bsrn pyranometers were calibrated 10 months earlier by Eppley using its method (Drummond and Greer 1966). The BORCAL is a clear-sky calibration that compares the sum of the direct horizontal irradiance, measured by a cavity radiometer, plus the diffuse horizontal irradiance, measured by a pyranometer under a tracking disk, to outputs of groups of pyranometers under test. All measurements made with the sun between 45° and 55° solar zenith angle are ratioed to these reference sums and averaged to determine the calibration of the test instruments. Eppley calibrates in an artificial sky containing incandescent bulbs distributed to uniformly illuminate a $BaSO_4$-coated housing from below the instrument's horizon and provide an irradiance level of about 700 W m^{-2} at the horizontal plane of the pyranometer. The output of a pyranometer under calibration is compared with the output of the reference pyranometer to derive a calibration. Their reference pyranometer is calibrated outdoors by shading and unshading the pyranometer and comparing voltage output differences to the direct horizontal irradiance measured by an AHF cavity radiometer near 45° solar zenith angle.

The shading/unshading technique for calibrating a pyranometer will lead to an underestimate of the responsivity of that pyranometer if the shade/unshade time is short relative to the time constants of the pyranometer.

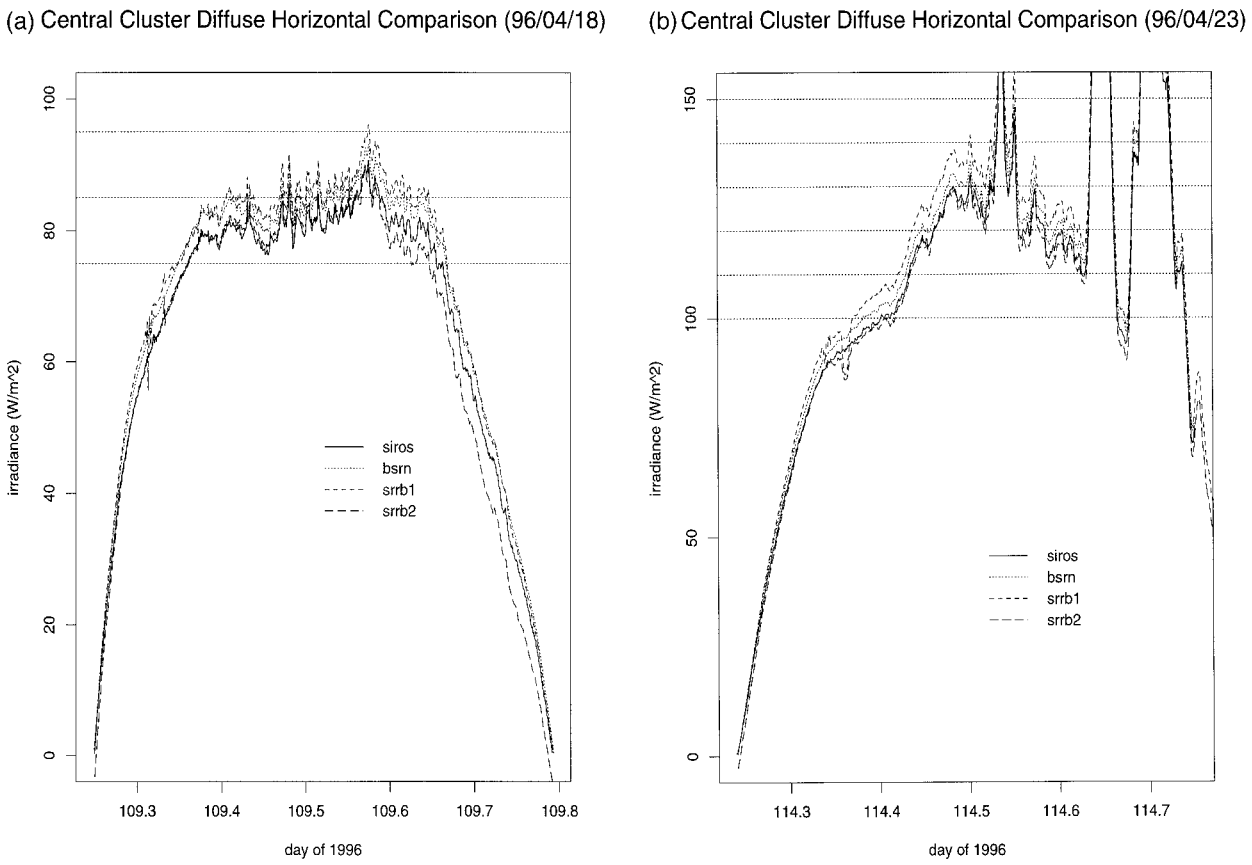

FIG. 10. (a) Diffuse horizontal irradiance (four pyranometers). (b) Diffuse horizontal irradiance (5 days later).

Wardle et al. (1996) explain that there is a secondary response time of minutes associated with the cooling and heating of pyranometer domes of the type used in this experiment that reduces the differences in the shade/unshade millivolt response range by between 1% and 2% for a 30-s shading sequence, for example. This reduced response range will lead to a responsivity (in V/W m^{-2}) that is too low and, consequently, irradiance measurements that are too high. However, the pyranometer whose calibration is traceable to a shade/unshade technique (siros) has an irradiance that is lower than the rest in Fig. 8, suggesting that larger systematic errors than discussed here dominate the differences seen in Fig. 8.

Figure 9a, similar to Fig. 8, is a plot of total horizontal irradiance for 23 April for five pyranometers. The ASRC pyranometer was added to the earlier group; it, too, was calibrated after the return from the SGP site by NREL using the BORCAL technique. Srrb1 and ASRC overlap so completely that it is difficult to distinguish the two. Although srrb1 clearly underestimates srrb2 near solar noon on 18 April, srrb1 and srrb2 differences on 23 April near solar noon are smaller, suggesting that minor variations may not be unexpected from day to day among these instruments. Siros and bsrn have a similar behavior relative to the SRRB pyranometers on both days. These features are better visualized in Fig. 9b, which expands Fig. 9a near solar noon.

Figure 10a is a plot of the diffuse horizontal irradiance on 18 April, and Fig. 10b is the diffuse plot for 23 April. The diffuse is higher on 23 April, indicating a brighter sky caused by higher aerosol loading and cirrus clouds, especially in the afternoon. Since the magnitude of the diffuse horizontal irradiance is smaller than the total horizontal irradiance, the spread in the diffuse horizontal irradiance tends to be much smaller, on the order of 10 W m^{-2}, rather than the 50–60 W m^{-2} measured by the total horizontal pyranometers of Figs. 8 and 9. This is a different set of pyranometers, and responses have shifted relative to the associated pyranometers used for total horizontal irradiance.

The most accurate measurement of solar radiation is the direct beam measured with an unwindowed absolute cavity radiometer. Typical uncertainties are 0.3% [Fröhlich (1991) and discussion in section 2] or about 3 W m^{-2} for clear-sky direct irradiances near solar noon. Figure 11a is a plot of the direct solar irradiance measured on 23 April with two SRRB cavity radiometers (srrb1 and srrb2), one ASRC Eppley NIP pyrheliometer (asrc) calibrated 1 week before the SGP experiment using an

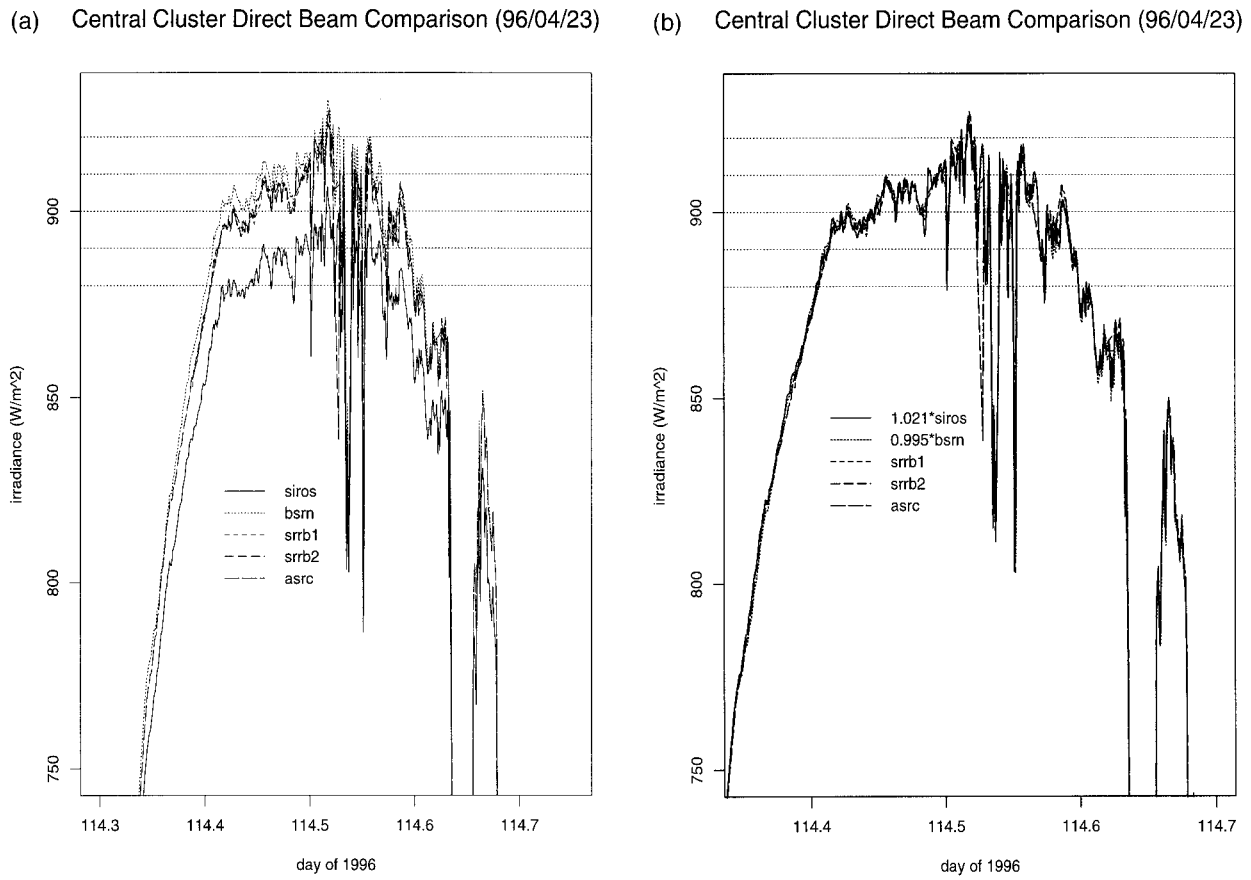

FIG. 11. (a) Direct normal irradiance (five pyrheliometers). (b) Same as (a) after calibration.

absolute cavity radiometer), and two Eppley NIP pyrheliometers (siros and bsrn) calibrated 19 and 33 months earlier using the BORCAL technique), which is a direct comparison to an absolute cavity radiometer. The two absolute cavity radiometers (srrb1 and srrb2) and the ASRC pyheliometer (asrc) track within 3 W m^{-2} throughout the day. Bsrn appears about 5 W m^{-2} high relative to this group in the morning and is closer in the afternoon. Siros is about 2% or 20 W m^{-2} low relative to the cavities throughout the day. The tracking for the siros pyrheliometer was observed to be highly reliable throughout the day. The tracking for the bsrn pyheliometer was not. It was near but not beyond the margin at which vignetting occurs for most of the day and slightly beyond that margin at which some vignetting occurs in the late afternoon. It is suggested that the apparently improved agreement in the afternoon is actually a slight loss of signal because of instrument pointing.

Since the latter two pyrheliometers, bsrn and siros, had missed their recommended annual recalibrations, we used the concurrent absolute cavity radiometer measurements on the morning of 23 April to calibrate the siros and bsrn pyrheliometers. This, in fact, is the recommended BORCAL procedure for calibrating pyrheliometers. Figure 11b shows remarkable agreement after adjusting the bsrn and siros units by the factors indicated in the legend in Fig. 11b. Agreement is now on the order of 3 W m^{-2} for all direct irradiance measurements on this day.

Again, the total horizontal irradiance is the diffuse horizontal irradiance plus the direct horizontal irradiance. These are sensed simultaneously by a pyranometer. However, all pyranometers show an angular response that is not a perfect cosine response; that is, the response does not decrease exactly as the cosine of the angle of incidence [Michalsky et al. (1995) and discussion in section 2]. We find that BORCAL and Eppley calibration factors for the same pyranometers typically show differences of 1.5%. Furthermore, pyranometers of the same manufacturer do not have exactly reproducible cosine responses.

Figure 11b demonstrates that direct irradiance can be measured reproducibly. Figure 10 illustrates that diffuse irradiance is small in magnitude, and the scatter in absolute terms among various instruments is low for clear-sky conditions. Therefore, a component sum of the latter two should be a better determination of the total horizontal irradiance.

Figure 12a is a plot of the summed components for

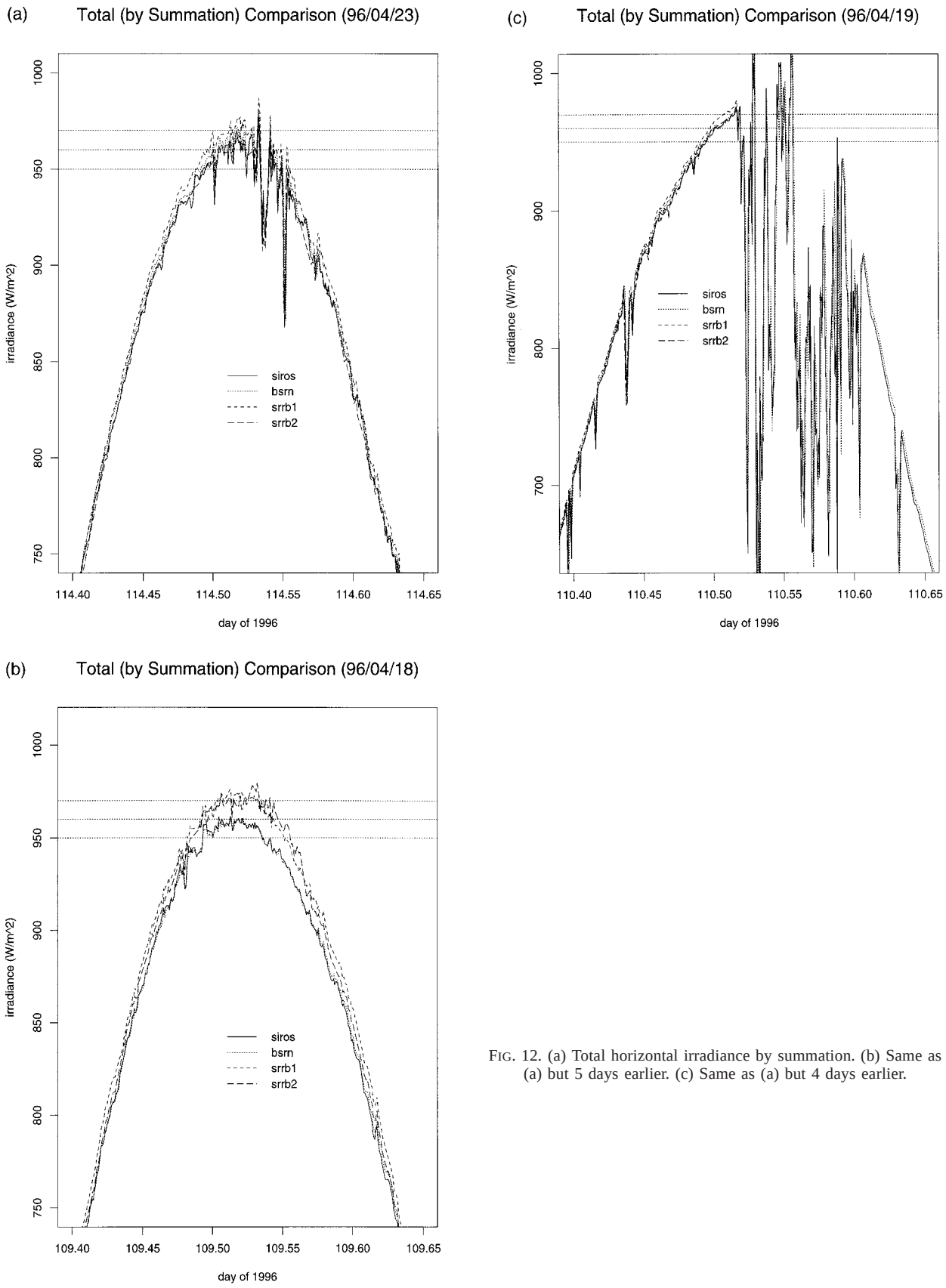

FIG. 12. (a) Total horizontal irradiance by summation. (b) Same as (a) but 5 days earlier. (c) Same as (a) but 4 days earlier.

four sets of instruments on 23 April using the new calibrations of the siros and bsrn pyrheliometers. Figure 12b is a similar plot for 18 April. These should be compared to Figs. 9b and 8b, respectively. The spread near solar noon in Fig. 12a is less than 10 W m^{-2} on 23 April compared to 60 W m^{-2} spread among the pyranometers in Fig. 9b. Figure 12b shows slightly more spread than Fig. 12a, but it is still small relative to the pyranometer measurements of total horizontal irradiance in Fig. 8b. Figure 12c shows a spread of the summed components on 19 April that is smaller than the data from either 18 or 23 April. The smallest morning aerosol loading of the three days occurs on 19 April, as indicated by the low variability in the morning time series data (neglecting the dips caused by small cloud passages).

4. Discussion

The most reproducible measurement of total horizontal irradiance is the sum of the direct horizontal irradiance plus the diffuse horizontal irradiance. Figure 12 indicates agreement among all four measurement sets throughout the three days to be about or better than 10 W m^{-2}.

The direct normal irradiance as shown in Fig. 11b agrees to within 3 W m^{-2} for all five instruments for 23 April. Equivalent results were obtained on 19 April, but the scatter was twice as large on 18 April, which gave rise to the larger spread in the total horizontal irradiance for that day.

Candidates for the remaining differences are tracking errors and dirty windows. The absolute cavity radiometer tracker for srrb2 was slightly misaligned on 18 April for about an hour just after solar noon. According to site protocol, the siros and bsrn instruments were checked and cleaned, *if needed*, each morning by site personnel; the srrb and asrc instruments were checked by the authors. Data not shown indicate that the siros and bsrn pyrheliometers were cleaned midmorning on 19 April (before the data shown in Fig. 12c and after the data shown in Fig. 12b), leading to an approximate 10 W m^{-2} increase in irradiance. We suspect that the differences in Fig. 12b on 18 April may have been caused by dust on the siros and bsrn pyrheliometer windows.

Three of the pyranometers used for the total horizontal irradiance measurements received calibrations after their return from the ARM site. In Fig. 9b these pyranometers agree to within about 10 W m^{-2}. It is probable that had the siros and bsrn total horizontal pyranometers been postcalibrated, then they too would fall nearer to this group. However, this group's mean solar noon reading is some 30 W m^{-2} higher than the summed totals in Fig. 12a. This higher reading at solar noon is consistent with the typical angular response of this pyranometer. The BORCAL calibration is performed at a mean solar zenith angle of 50°. At solar noon in late April the sun has a solar zenith angle around 25°. Eppley PSP thermopile pyranometers often have angular responses that move farther (lower) from a true cosine response as the angle of incidence increases [see Figs. 1 and 5 in Michalsky et al. (1995)]. This implies that a calibration constant obtained for an incidence angle of 50°, where the instrument is less sensitive, will yield an irradiance response that is higher than it should be at smaller angles of incidence, where it is more sensitive—that is, solar noon in late April at the SGP site.

What about the pyranometer measurement of diffuse horizontal irradiance? Are they any better than total horizontal irradiance measurements? The radiation contribution of the sky hemisphere to a flat plate horizontal Lambertian receiver—for example, a pyranometer—is proportional to sin(2 × solar zenith angle). This function peaks at 45° and falls to zero at 0° and 90°; the BORCAL calibration near 50° is approximately correct for an isotropic sky radiator, although 45° is the preferred angle. For the Eppley instrument whose cosine response relative to the perfect receiver decreases monotonically at higher angles of incidence, the calibration at 45° is sensitive to the largest contribution of sky radiation and is too high relative to radiation received at lower angles of incidence and too low relative to radiation received at higher angles of incidence, thereby achieving some balance through offsetting errors. The sky radiance is not isotropic; therefore, a pyranometer with an imperfect angular response will still have some error, but this should minimize it for the general case.

In conclusion, as suggested by the World Climate Research Program's BSRN, we recommend the sum of the direct horizontal irradiance plus the diffuse horizontal irradiance as the best measure of total horizontal irradiance. With frequently calibrated instruments and daily cleaning, this has been achieved for some measurements at the ARM site. We recommend these measurements for model comparisons of total and diffuse horizontal and direct normal shortwave irradiance.

Acknowledgments. Rudy Haas, Dave Longenecker, and Jim Wendell were crucial to the successful data collection phase of the comparison at CMDL. This research was funded in part by the Atmospheric Radiation Measurement program of the U.S. Department of Energy; the Office of Energy Research; the Office of Biological and Environmental Research; the Environmental Sciences Division by Grant DE-FG02-90ER61072 (SUNY), Contract W-31-109-Eng-38 (Argonne), Battelle Contract 164514-A-Q-1 (CIRES, SRRB), Contract DE-AC36-83CH10093 (NREL), and Battelle Contract 144880-A-Q-1 (Oklahoma); and in part by the NOAA, Climate Monitoring and Diagnostics Laboratory.

REFERENCES

Betts, A. K., J. H. Ball, and A. C. M. Beljaars, 1993: Comparison between the land surface response of the ECMWF model and the FIFE-1987 data. *Quart. J. Roy. Meteor. Soc.*, **119,** 975–1001.

Cess, R. D., M. H. Zhang, Y. Zhou, X. Jing, and V. Dvortsov, 1996: Absorption of solar radiation by clouds: Interpretations of satellite, surface and aircraft measurements. *J. Geophys. Res.,* **101,** 23 299–23 309.

Charlock, T. P., and T. L. Alberta, 1996: The CERES/ARM/GEWEX experiment (CAGEX) for the retrieval of radiative fluxes with satellite data. *Bull. Amer. Meteor. Soc.,* **77,** 2673–2683.

Ding, M., and W.-C. Wang, 1996: GCM radiation model-to-observation comparison. *Proc. Seventh Symp. on Global Change Studies,* Atlanta, GA, Amer. Meteor. Soc., 141–145.

Drummond, A. J., and H. W. Greer, 1966: An integrating hemisphere for the calibration of meteorological pyranometers. *Sol. Energy,* **10,** 7–11.

Flowers, E. C., and E. L. Maxwell, 1986: Characteristics of network measurements. *Sol. Cells,* **18,** 205–212.

Fröhlich, C., 1978: *WMO Final Rep.,* **490,** 108–112.

——, 1991: *Metrologia,* **28,** 111–115.

Fu, Q., and K.-N. Liou, 1993: Parameterization of the properties of cirrus clouds. *J. Atmos. Sci.,* **50,** 2008–2025.

Kato, S., T. P. Ackerman, C. N. Long, E. E. Clothiaux, and J. H. Mather, 1996: A comparison between clear-sky shortwave flux calculations and observations during ARESE. *Proc. Sixth Atmospheric Radiation Measurement Science Team Meeting,* San Antonio, TX, United States Department of Energy, 39–40.

Michalsky, J. J., L. C. Harrison, and W. E. Berkheiser III, 1995: Cosine response characteristics of some radiometric and photometric sensors. *Sol. Energy,* **54,** 397–402.

Myers, D. R., K. Emery, and T. L. Stoffel, 1989: Uncertainty estimates for global solar irradiance measurements used to evaluate PV device performance. *Sol. Cells,* **27,** 455–464.

Ohmura, A., and Coauthors, 1998: Baseline surface radiation network (BSRN/WCRP): New precision radiometry for climate research. *Bull. Amer. Meteor. Soc.,* **79,** 2115–2136.

Toon, O. B., C. P. Mckay, and T. P. Ackerman, 1989: Rapid calculation of radiative heating rates and photodissociation rates in inhomogeneous multiple scattering atmospheres. *J. Geophys. Res.,* **94,** 16 287–16 301.

Wardle, D. I., and Coauthors, 1996: Improved measurements of solar irradiance by means of detailed pyranometer characterization. International Energy Agency Rep. IEA-SHCP-9C-2, 217 pp. [Available from National Atmospheric Radiation Centre, Atmospheric Environment Service, 4905 Dufferin Street, Downsview ON M3H 5Y4, Canada.]

Wild, M., A. Ohmura, H. Gilgen, and E. Roeckner, 1995: Validation of general circulation model radiative results using surface observations. *J. Climate,* **8,** 1309–1324.

Zender, C. S., B. Bush, S. K. Pope, A. Bucholtz, W. D. Collins, J. T. Kiehl, F. P. J. Valero, and J. Vitko Jr., 1997: Atmospheric absorption during the Atmospheric Radiation Measurement (ARM) Enhanced Shortwave Experiment (ARESE). *J. Geophys. Res.,* **102,** 29 901–29 915.